Eur Biophys J (2002) 30: 559–570
DOI 10.1007/s00249-001-0193-z

ARTICLE

**Carmelo La Rosa · Danilo Milardi
Domenico M. Grasso · Martin P. Verbeet
Gerard W. Canters · Luigi Sportelli · Rita Guzzi**

A model for the thermal unfolding of amicyanin

Received: 16 May 2001 / Revised version: 18 September 2001 / Accepted: 1 October 2001 / Published online: 24 November 2001

Abstract In the present study the thermal unfolding of amicyanin has been addressed using differential scanning calorimetry, fluorescence emission, optical density, circular dichroism and electron paramagnetic resonance. The combined use of these techniques has allowed us to assess, during unfolding of the protein, its global conformational changes in relationship to the local structural modifications occurring in the copper environment and close to the fluorescent chromophore Trp46 of the protein. The thermal transition from the native to the denatured state is on the whole irreversible and occurs in the temperature range between 65 and 72 °C, depending on the scan rate and technique used. Amicyanin as a whole shows a complex unfolding pathway, which has been described in terms of a three-step model: $N \rightleftharpoons U \rightarrow F_1 \rightarrow F_2$. According to this model, in the first step the native state of the protein (N) goes reversibly to the unfolded state (U), in the second one U goes irreversibly to F_1 and, finally, the state F_2 is irreversibly reached in the third step. Kinetic factors prevent the experimental separation of these steps. Nevertheless, the comparison of the data obtained with the different experimental techniques testifies the presence, within the unfolding pathway, of some intermediate states, although not sufficiently long-lived to allow a detailed characterization. A first intermediate transient state has been identified around 68 °C, whereas a second one can be related to conformational changes that involve the copper environment. Finally, an exothermal phenomenon, caused by irreversible rearrangements of the melted polypeptide chains, is evidenced. In addition, according to the EPR findings, the type 1 copper ion, which is four-fold coordinated by two N and two S atoms in a distorted tetrahedron in the native state of the protein, shows type 2 features after denaturation. A mathematical model simulating the unfolding Cp_{exc} profile has been also developed.

Keywords Amicyanin · Thermal unfolding · Intermediates · Thermodynamics · Irreversibility

C. La Rosa (✉) · D. Milardi · D.M. Grasso
Dipartimento di Scienze Chimiche,
Università di Catania, V.le A. Doria 6, 95125 Catania, Italy
E-mail: clarosa@dipchi.unict.it
Tel.: +39-95-7385114
Fax: +39-95-580138

M.P. Verbeet · G.W. Canters
Leiden Institute of Chemistry,
Gorleaus Laboratories, Leiden University,
P.O. Box 9502, 2300 RA Leiden, The Netherlands

L. Sportelli · R. Guzzi
Dipartimento di Fisica e Unità INFM,
Laboratorio di Biofisica Molecolare,
Università della Calabria, 87036 Arcavacata di Rende (CS), Italy

Introduction

The blue copper proteins are widely recognized to have a number of remarkable spectroscopic and chemical properties, including intense low-energy electronic absorption features in the visible spectrum, small hyperfine coupling constants in the EPR spectra and fast electron transfer dynamics (Malkin and Malmstrom 1970; Fee 1975). However, in spite of the intense investigations carried out on these systems, many important aspects remain to be understood. As an example, the relationships between the structural features of these proteins, their thermodynamic stability and/or their unfolding mechanism need to be elucidated. A major goal of experimental work addressing this problem is to detect and to characterize partially folded states, including transient intermediates as observed in kinetic experiments and stable intermediates occurring under equilibrium conditions. Despite the wealth of structural data that are by now available from X-ray, NMR and molecular dynamics studies, the lack of exhaustive thermodynamic information concerning the folding/unfolding equilibrium prevents us to fully elucidate all the aspects of the process.

Among blue copper proteins, amicyanin (Tobari and Harada 1981; Tobari 1984; Husain and Davidson 1985; Lawton and Anthony 1985) shows intriguing, unique

structural features. The three-dimensional structure of amicyanin from *Paracoccus versutus* is known in detail by both X-ray diffraction (Romero et al. 1994) and NMR studies on the protein in solution (Kalverda et al. 1994). The overall structure of the protein can be described as a β-sandwich, essentially formed by eight β-strands arranged in two sheets. Almost 30% of the residues are involved in forming β-turns. Even if this is the common folding topology of blue copper proteins, such as plastocyanin and azurin, whose thermal unfolding has been recently elucidated (La Rosa at al. 1995; Milardi et al. 1996, 1998), some differences can be observed. The main structural feature of amicyanin is the existence of a large 21-residue-long N-terminal chain that forms an extra β-strand not present in plastocyanin and azurin. The second difference concerns the loop which in azurin contains the α-helix and in plastocyanin the acidic patch. In amicyanin this region is not acidic and contains no α-helical structure. The copper ion is located between three loops at one end of the molecule (the so-called ''northern end'') and is coordinated by two N atoms from His54 and His96 and two S atoms from Cys93 and Met99 in a distorted tetrahedral geometry. In addition, Trp46 is located in the core of the protein, being an excellent, built-in, fluorescent probe. Such an unusual three-dimensional arrangement of amicyanin suggests that the unfolding pathway of this protein could be different from that of the cupredoxins studied previously.

Different experimental techniques have been used in the present work to investigate the folding/unfolding process of amicyanin, paying also attention to the structural features of the protein along the unfolding pathway. The results have shown the complex nature of the temperature-induced transition from the native to the fully denatured state of amicyanin, and also evidenced the presence of transient intermediate states. Subsequently, an extrapolation procedure of calorimetric curves to infinite scan rate (Freire et al. 1987; La Rosa et al. 1998) was applied to the amicyanin unfolding curves in order to extract the thermodynamic functions from the irreversible differential scanning calorimetry (DSC) transitions. As a result the thermal unfolding of amicyanin can be described by a complex model in which a reversible step is followed by two irreversible steps. A detailed mathematical analysis of the unfolding process, in combination with the development of an appropriate fitting program of the excess heat capacity (Cp_{exc}) curves, has demonstrated the correctness of the model proposed.

Materials and methods

Sample preparation

Paracoccus versutus amicyanin was obtained via overexpression in *Escherichia coli* strain JM109. For the expression and purification of the recombinant amicyanin, a standardized protocol was followed as previously described (Van Houwelingen et al. 1985; Kalverda et al. 1994). Throughout the experiments, only fully oxidized amicyanin was used. The protein was diluted in the same buffer as used for dialysis, 10 mM phosphate buffer solution (PBS), pH 7 (0.1 M ionic strength).

Differential scanning calorimetry

DSC scans were carried out with a SETARAM (Lyon, France) microDSC III with stainless steel 1 mL sample cells. The temperature resolution is 0.01 °C. The instrument sensitivity is 90 $\mu V\ mW^{-1}$. The same solution without the protein was used in the reference cell. Experiments involving protein concentrations in the range from 0.8 to 2 mg mL^{-1} have shown that the DSC transitions do not depend on protein concentration (data not shown). As a consequence, the amicyanin concentration used in all the experiments was 1.5×10^{-4} M. Both the sample and the reference (PBS) were scanned from 30 to 100 °C with a precision of ±0.02 °C at scanning rates of 0.3, 0.5, 0.7 and 1.0 K min^{-1}. Electric signals coming from the DSC were collected, starting from the point at which a stable baseline was obtained. In order to obtain the Cp_{exc} curves, buffer-buffer base lines were obtained at the same scanning rate and then subtracted from the sample curves according to a previously established procedure (La Rosa et al. 1995). All the Cp_{exc} curves were obtained using a fourth-order polynomial fit as baseline. The average level of noise was about ±0.4 μW and the reproducibility at refilling was about 0.1 mJ K^{-1} mL^{-1}. Calibration in energy was obtained by providing a well-defined amount of power input, electrically generated by an EJ2 SETARAM Joule calibrator within the sample cell.

Optical density

OD measurements were carried out with a JASCO 7850 spectrophotometer equipped with a Peltier-type thermostated cell holder (model EHC-441) and a temperature programmer (model TPU-436; precision ±0.2 °C). The protein concentration was 2.5×10^{-5} M. The temperature was scanned from 30 to 90 °C at the same scanning rates as used in the DSC measurements.

Fluorescence emission

Fluorescence emission curves were acquired with a Perkin-Elmer LS 50B spectrofluorimeter equipped with a Peltier Temperature Programmer PTP-1. The excitation wavelength was 295 nm, while the excitation and emission band-passes were 6 and 4 nm, respectively. Protein samples were scanned from 30 to 85 °C at 0.5 K min^{-1}. The temperature of the samples was measured directly by a YSI precision thermistor dipped in the cuvette. The emission spectra were recorded at a scan speed of 400 nm min^{-1}. The protein concentration was 2.5×10^{-5} M.

Circular dichroism

CD measurements in the far-UV region (200–330 nm) were performed with a JASCO 700 spectropolarimeter using quartz cuvettes of 0.1 cm optical path. The amicyanin concentration was 3.8×10^{-5} M.

Electron paramagnetic resonance

The EPR measurements were carried out with a Bruker ER 200D-SRC X-band spectrometer equipped with the ESP 1600 Data System. The EPR spectra were recorded at 77 K by plunging the sample solution in a finger Dewar containing liquid nitrogen. The concentration of amicyanin was about 10^{-3} M.

Results

Differential scanning calorimetry

In Fig. 1a the Cp_{exc} profile of amicyanin at the scan rate of 0.5 K min^{-1} is shown. The amicyanin Cp_{exc} profile shows two overlapping endothermic peaks centred at $T_m = 68.4$ and $T_m = 74.2$ °C and an exothermic one located at the end of the thermal transition at approximately $T_m = 78.5$ °C, where T_m is defined as the maximum heat capacity temperature of the calorimetric peak.

In order to understand the origin of the two overlapping endotherms in the DSC thermogram, protein samples were scanned at the heating rate of 0.5 K min^{-1} according to the following heating/cooling cycles. (1) Heating from 30 to 100 °C (Fig. 2a, dotted line) and subsequent rapid cooling to 30 °C. A second run of this sample in the same temperature range did not show any endotherm (Fig. 2a, solid line). (2) Heating from 30 to 68.4 °C (Fig. 2b, dotted line) and rapid cooling to 30 °C. When the same sample was re-heated up to 100 °C (Fig. 2b, solid line) a partial reversibility of the thermally induced process was observed. (3) A third protein sample was then heated from 30 to 74.2 °C (Fig. 2c, dotted line) and again rapidly cooled to 30 °C. No heat absorption was observed in the second heating cycle of this sample (Fig. 2c, solid line).

The results of these thermal cycles ensure that the thermal unfolding of amicyanin is, on the whole, irreversible and it cannot be directly analysed in the light of equilibrium thermodynamics. The presence of kinetic factors within the unfolding process of amicyanin can be evidenced by performing DSC scans at different scan rates and constant protein concentration. The DSC scans of amicyanin obtained at 0.3, 0.5, 0.7 and 1.0 K min^{-1} are shown in Fig. 3a. Each DSC profile was

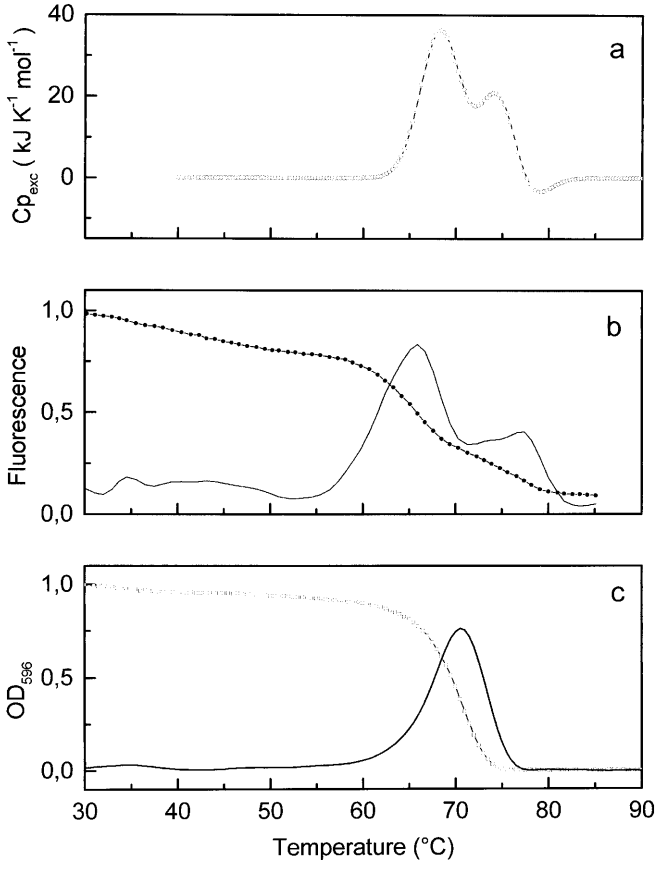

Fig. 1a–c Experimental thermal profiles of amicyanin in PBS recorded at 0.5 K min^{-1}. **a** DSC. **b** Normalized intensity of the fluorescence emission at 314 nm (*filled circles*) ($\lambda_{exc} = 295$ nm). The negative of the first derivative of the normalized fluorescence with respect to the temperature (*solid line*) is also shown. **c** Normalized optical density at 596 nm (*open squares*) and the negative of the first derivative with respect to the temperature (*solid line*)

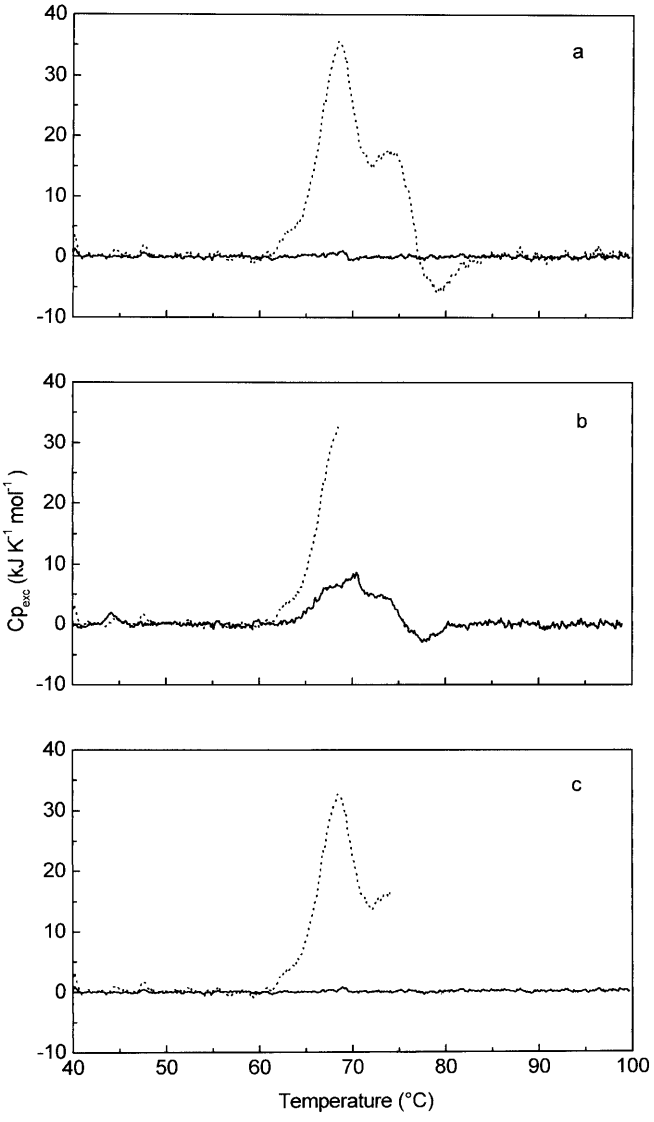

Fig. 2 DSC profiles (*dotted line*) of amicyanin heated up to **a** 100 °C, **b** 68.4 °C and **c** 74.2 °C. The rescan obtained after cooling the samples to 30 °C (*solid lines*) are shown. The scan rate was 0.5 K min^{-1} for each heating scan

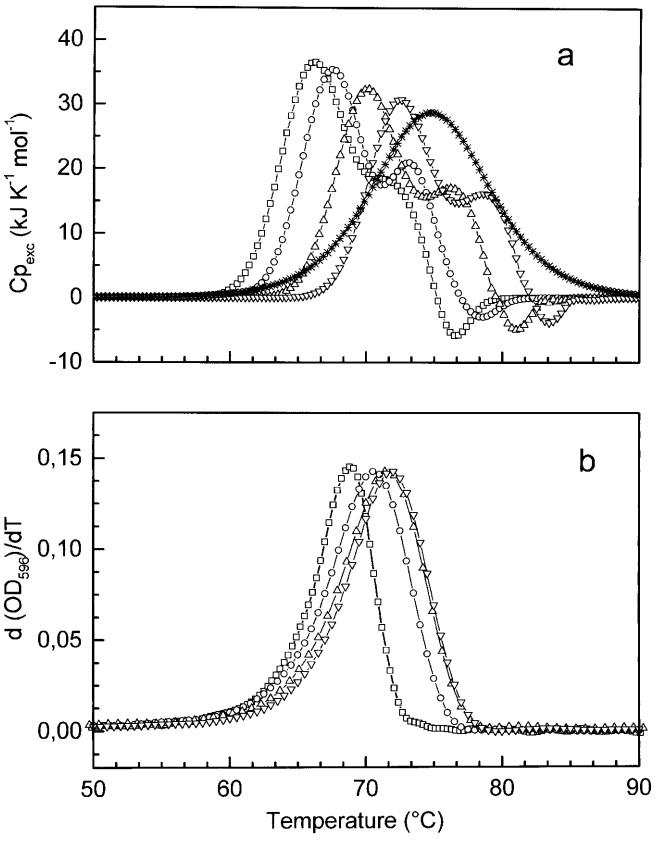

Fig. 3 Scan rate effect **a** on the DSC profile and **b** on the negative of the first derivative of the optical density at 596 nm with respect to the temperature of amicyanin. The scan rates are: (*squares*) 0.3 K min^{-1}, (*circles*) 0.5 K min^{-1}, (*triangles*) 0.7 K min^{-1} and (*down triangles*) 1.0 K min^{-1}. The extrapolated Cp_{exc} curve (*stars*) obtained as described in the text is also shown. The transition temperatures (T_t) observed for the optically detected thermal transition were 68.8, 70.5, 71.4 and 72 °C for curves obtained at 0.3, 0.5, 0.7 and 1.0 K min^{-1}, respectively

deconvoluted in three Gaussian components and the results are given in Table 1. From the data reported in Table 1 it can be noted that all the T_m values increase with the scan rate. It is also evident that the first component is in any case the major contribution to the overall calorimetric enthalpy.

The thermal profiles shift to higher temperature with the increase of the scan rate. According to a previously published paper (Sanchez-Ruiz 1992), DSC runs performed at different protein concentrations provide an effective test to establish if changes in molecularity of the unfolding process can occur. In the case of amicyanin, a change of molecularity during heating is unlikely because no change in enthalpy or temperature of maximum heat absorption, T_m, were observed in experiments at different protein concentrations (data not shown).

Fluorescence emission

Amicyanin has a single tryptophan (Trp46) residue buried in a hydrophobic and inner region of the protein (Kalverda et al. 1994). Because of its localization, the Trp residue can be considered a powerful probe to monitor the structural changes occurring in the protein as the temperature is increased. At room temperature, amicyanin shows a maximum fluorescence emission at $\lambda_{max} = 314$ nm, which is compatible with a Trp residue in a hydrophobic environment (Lakowicz 1983). The intensity of emission at this wavelength decreases with temperature because the Trp residue will be exposed to a more polar environment once the unfolding takes place. Thus, λ_{max} shifts to 357 nm. Figure 1b (filled circles) shows the variation of the normalized fluorescence emission at 314 nm as a function of the temperature at the scan rate of 0.5 K min^{-1}. If the fluorescence thermal profile is drawn in terms of the negative of the first derivative of the experimental points with respect to the temperature (Fig. 1b, solid line), two peaks corresponding to two transitions are observed. The temperature of the first peak, T_f, is 66 °C whereas the second is centred at 78 °C.

Optical density

The copper site in amicyanin lies in a cavity formed by four β-strands shielded from the solvent. The His96 is the only ligand residue which is partially surface exposed. The most distinctive feature of a type 1 copper site is its intense blue colour which, in amicyanin, originates from a ligand-to-metal charge transfer transition from the Cys93 to the copper ion, centred at 596 nm.

Table 1 Scan rate effect on amicyanin DSC thermograms. The three components of the Cp_{exc} curves were obtained using simple Gaussian peaks. Amicyanin concentration was 1.5×10^{-4} M in PBS. T_m in °C and ΔH in kJ mol^{-1}

v (K min^{-1})	1st component		2nd component		3rd component		Overall		
	T_m (°C)	ΔH (kJ mol^{-1})	T_m (°C)	ΔH (kJ mol^{-1})	T_m (°C)	ΔH (kJ mol^{-1})	T_m (°C)	ΔH (kJ mol^{-1})	$\Delta H^{cal}/\Delta H^{VH}$
0.3	66.1	214	72.1	87	76.2	–24	–	277 ± 14	–
0.5	67.5	197	73.3	82	78.3	–10	–	269 ± 16	–
0.7	70.0	182	76.5	92	80.3	–26	–	247 ± 16	–
1	72.5	175	78.7	79	82.9	–15	–	238 ± 19	–
∞[a]	–	–	–	–	–	–	74.7 ± 0.1	331 ± 11	1.03

[a]Extrapolated values were obtained as reported in the text

For this peculiar property this site can be considered as a good reporter of the thermally induced local modification occurring in correspondence to the copper environment. Figure 1c shows the variation of the normalized optical density at a fixed wavelength ($\lambda = 596$ nm) of amicyanin in PBS between 30 and 90 °C (OD_{596}/T) at a scan rate of 0.5 K min^{-1} (open squares). The negative of the first derivative of the OD_{596}/T profile (Fig. 1c, solid line) allows us to calculate with high accuracy the transition temperature, T_t, as 70.5 °C. The symmetry of the curve suggests that the disruption of the copper environment can be described by a "two-state" path. The denaturation process of amicyanin is accompanied by the bleaching of the protein solution and the blue colour is no longer recovered by cooling the sample to room temperature. Consequently, the visible absorption spectrum of a previous denatured sample shows only a residual absorption which, at 596 nm, has the same value over all the temperature range. Thus, similarly to the DSC results, visible absorption reveals an irreversible thermal transition. This irreversibility can be partially eliminated, if the thermal transition of the sample scanned at 0.5 K min^{-1} is stopped at 70 °C and then rapidly cooled to room temperature. In fact, under this condition the native absorption is partially recovered. This finding is in agreement with the corresponding DSC thermal cycle (Fig. 2b), suggesting a close correlation between the second DSC endothermic peak and the "disruption" of the copper environment.

In order to elucidate the dependence of OD_{596}/T profile on the scan rate, the negatives of the first derivatives of OD_{596}/T are shown in Fig. 3b. The effect of the increasing scan rate is to shift T_t to higher temperatures, while the symmetry of the curves is maintained. Such an effect, which has been already observed in the DSC profiles, suggests the presence of kinetic factors within the unfolding pathway of amicyanin. From the scanning rate effect on both DSC thermograms and OD_{596}/T curves it is possible to extract kinetic information related to the thermal unfolding of amicyanin. In particular, by using the equation (Sanchez-Ruiz 1992): $ln(v/T_i^2) = C - E_{app}/RT_i$, where v is the scan rate (°C min^{-1}), T_i is the transition temperature, T_m or T_t of the corresponding profiles and C is a constant, it is possible to calculate the apparent activation energy, E_{app}, of the thermally induced processes. According to this equation, for the two endothermic components of the DSC thermogram we have obtained $E_{app1} = 174 \pm 9$ kJ mol^{-1} for the first component, and $E_{app2} = 172 \pm 10$ kJ mol^{-1} for the second component. Similarly, if this criterion is applied to the optical data in Fig. 3b, an apparent activation energy of $E_{app} = 333 \pm 24$ kJ mol^{-1} is obtained.

Differences in the apparent activation energies calculated by means of optical and calorimetric experiments are quite normal for blue copper proteins and have been already observed for azurin and plastocyanin (La Rosa et al. 1995; Milardi et al. 1998). These differences can be ascribed to the fact that spectroscopic investigations are limited to a well-defined spatial region of the protein, i.e. the active site; calorimetric measurements involve the whole structure of the protein and of course the kinetics of the observed phenomena are different.

Electron paramagnetic resonance

Figure 4 shows the EPR spectra of amicyanin in aqueous solution recorded at 77 K in the (a) native and (b) denatured states. The spectral features of native amicyanin are typical of a type 1 copper ion with axial symmetry characterized by four hyperfine lines centred at $g_{||} = 2.235$ and separated by $A_{||} = 58\times10^{-4}$ cm^{-1} in the low magnetic field region. The small separation of the hyperfine lines in the high-field region, $A_{\perp} = 4.8\times10^{-4}$ cm^{-1}, is responsible for their appearance as a single intense resonance line centred at $g_{\perp} = 2.042$ (Van Houwelingen et al. 1985). The values of the magnetic parameters describing the low-field region of the spectrum are directly derived from the experimental spectrum, while the high-field region parameters have been obtained from the simulation of the experimental spectrum (data not shown).

To obtain the denatured state of the protein, the solution has been maintained at 75 °C, until the blue colour disappears (about 10 min). The EPR spectrum of this sample, recorded under the same experimental conditions as the native protein, is shown in Fig. 4, line b. The same result is obtained if the protein solution is heated to 100 °C and then cooled. This spectrum is characterized by a large increase of $A_{||}$ to 187×10^{-4} cm^{-1} in the high-field region. Slight variations of the g-values with respect to the native state are found. The magnetic values characterizing the EPR spectrum of denatured amicyanin are compatible with a type 2 copper site with a square-planar coordination of the copper. Based on the correlation map of $A_{||}$ versus $g_{||}$ for a series of copper complexes (Addison 1983), the copper ligands of

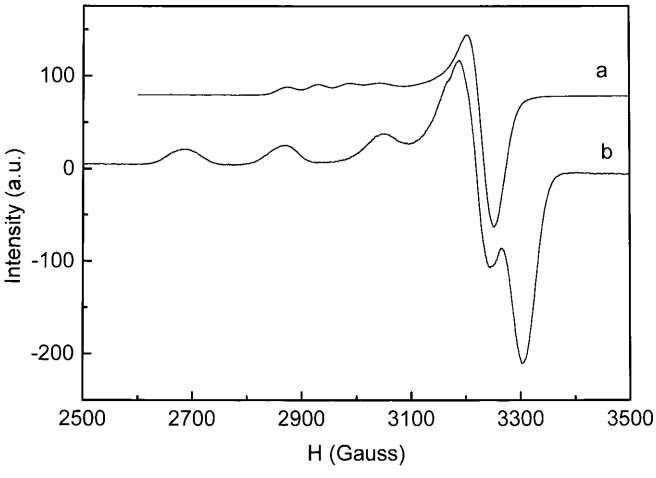

Fig. 4 EPR spectra of amicyanin in PBS recorded at 77 K: *a* native state; *b* after heating at 75 °C

amicyanin in the denatured state are identified as two nitrogen and two oxygen atoms. A similar result has previously been found for azurin (La Rosa et al. 1995) and plastocyanin (Milardi et al. 1998). Differently, Leckner et al. (1997) have observed a change in the oxidation of the copper ion ($Cu^{2+} \rightarrow Cu^{+}$), which is magnetically silent, for acid-induced denaturation of azurin. The different method to induce protein denaturation may be responsible for the disagreement of the two final results.

Circular dichroism

The simplest method of extracting the secondary structure content from CD data is to assume that a spectrum is a linear combination of the CD spectra of each contributing secondary structure type (''pure'' α-helix, ''pure'' β-strand, etc.), weighted by its abundance in the polypeptide conformation. The major drawback of this approach is that there are no standard reference CD spectra for ''pure'' secondary structures. In response to these shortcomings, several methods have been developed to analyse experimental CD spectra using a database of reference protein CD spectra containing known amounts of secondary structures (Hennessey and Johnson 1981; Provencher and Glockner 1981; Manalevan and Johnson1987; Sreerama and Woody 1994). These methods are in general more accurate and reliable than the novel approach mentioned first, but accurate CD spectra at wavelengths < 200 nm are needed. For all these reasons we decided to analyse only qualitatively the CD spectra of different amicyanin samples, which are available starting from 200 nm. Figure 5 shows the CD spectra between 200 and 260 nm for amicyanin in PBS measured at room temperature on native and preheated protein samples. If no α-helix structures are present in the native molecule, the β-turns, β-sheets and random coil structures are located at 205 nm ($\Delta\epsilon > 0$), 218 nm ($\Delta\epsilon < 0$) and 230 nm ($\Delta\epsilon > 0$), respectively (Bohm et al. 1992). This assignment fits very well with the spectral features of the CD spectrum of amicyanin in the native state shown in Fig. 5 (solid line). It is interesting to note that if the protein solution is heated to 68.4 °C, corresponding to the melting temperature of the first peak in the DSC profile (Fig. 1a), the β-turn region of the CD spectrum disappears (Fig. 5, dashed line), whereas the β-sheet region is still evident. A direct conclusion can be that the first calorimetric peak is mainly ascribable to the denaturation of β-turns, while the β-sheets appear less affected. Moreover, at the same temperature the copper site has lost about 30% of its optical absorbance, although in a reversible way (Fig. 1c). On the other hand, if amicyanin is heated to 74.2 °C, corresponding to the second peak in the DSC curve, the CD signal (Fig. 5, dotted line) is very similar to the one obtained when amicyanin is completely denatured (Fig. 5, dashed-dotted line) reaching, presumably, a random coil-like configuration. This transition is irreversible and involves also the complete disruption of the copper site.

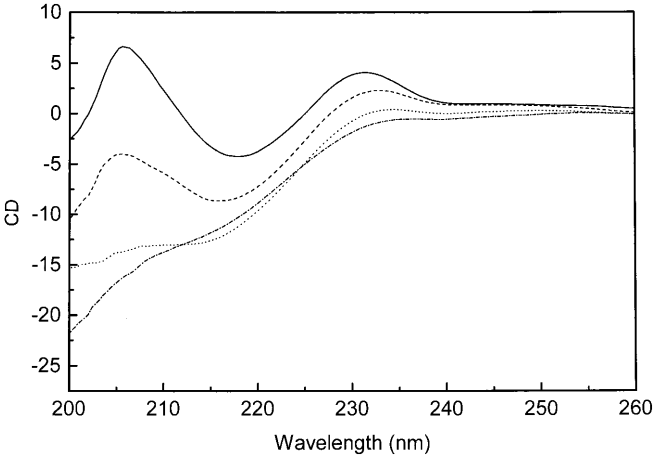

Fig. 5 CD spectra recorded at room temperature on amicyanin samples with different thermal histories. Native state (*solid line*), after heating at 68.4 °C (*dashed line*), after heating at 74.2 °C (*dotted line*) and a fully denatured amicyanin sample (*dotted and dashed line*)

Discussion

The main goal of performing thermal studies on proteins is to provide information about the energetics and the mechanism of unfolding. This, in turn, is believed to be informative in the understanding of how a polypeptide chain folds into a functionally active unique conformation. The complexity of such a process suggests that it may proceed through a definite sequence of intermediate states characterized by decreasing Gibbs free energy energies. Since these intermediates are often too unstable and short lived to be observed experimentally, their nature has been widely debated. However, some proteins, under certain conditions, assume conformations which can be distinguished from the native or completely unfolded states (Tanford 1968; Ptitsyn 1992). These cases have received particular attention, since they might provide a clue to the folding mechanism. While it is quite clear that the folding of large proteins proceeds in discrete steps corresponding to the folding of individual domains (Wetlaufer 1973; Privalov 1982; Novokhatny et al. 1984; Jaenicke 1991; Garel 1992; Abkevich et al. 1995; Dobson 1995), understanding the folding of a small protein without an evident subdomain organization remains a challenge. In this light, the study of thermal unfolding of amicyanin is of high interest. According to the experimental evidence reported in the present paper, at least two different intermediate states are involved. The populations of these states are under kinetic control and they are influenced differently by the heating rate. When the heating rate is increased, all thermal transitions tend to occur simultaneously. However, even if each intermediate is, under the experimental conditions adopted in the

present work, kinetically controlled, some transient states are sufficiently long lived to allow their spectroscopic detection. In particular, the first intermediate state is obtained in a partially reversible way and, as fluorescence emission studies confirm, it is accompanied by large motions of the Trp environment. CD measurements have shown that β-turns are the elements of the secondary structure most involved in this transformation. In this first intermediate state the copper environment appears similar to the native state, as optical measurements indicate. Moreover, the thermal effect associated with the transition from the native to the first intermediate state is the largest of all the DSC transitions. It is noteworthy to underline that the first intermediate state must not be confused with the unfolded state (U) depicted in the denaturation model $N \rightleftharpoons U \rightarrow F_1 \rightarrow F_2$. In fact the unfolded state of the protein can be approached only when heating rate is infinite. On the other hand, the transient intermediate states can be detected only at low scan rates. After this first intermediate, the Trp46 environment changes its conformation into a less rigid one. Optical and EPR findings clearly show that the copper environment is thoroughly and irreversibly modified during this conformational transition. In fact, in a sample analysed after a thermal treatment up to the temperature of the second DSC peak, instead of an axial type 1 symmetry the copper ion shows a planar geometry. The last step, characterized by a slightly exothermal DSC peak, is attributed to the occurrence of irreversible inter- or intramolecular interactions between the molten polypeptide chains.

A detailed thermodynamic analysis can be carried out only for the overall transition between the initial or native (N) and the unfolded (U) state. In this respect, it is essential to calculate the denaturational $\Delta H(T)$, $\Delta S(T)$ and $\Delta G(T)$ thermodynamic functions which, in turn, depend on ΔH_U, $T_{1/2}$ and $\Delta Cp = C_{p,U} - C_{p,N}$. Only in the case of a reversible transition can these parameters be directly extracted from the experimental DSC profiles. However, it has been recently shown that even for an irreversible transition the reversible component can be obtained by means of the extrapolation of the calorimetric curve at infinite scan rate (Freire et al. 1987; La Rosa et al. 1998). Since the exothermic peak decreases with increasing scan rate (Fig. 3 panel a), we can conclude that this exothermic contribution is time dependent. It is therefore reasonable to consider the reversible step separable from the irreversible one by means of the extrapolation of the calorimetric curves to infinite scanning rate (Freire et al. 1987).

The Cp_{exc} curve at infinite scanning rate was obtained by means of the following procedure: the cumulative enthalpy functions $<\Delta H>$ were calculated from the experimental calorimetric profiles obtained at different scan rates by using the equation:

$$\langle \Delta H \rangle = \int_{T_0}^{T} Cp_{exc} \mathrm{d}T \tag{1}$$

where T_0 is the temperature at which all molecules are in the initial state, and Cp_{exc} is the specific excess heat capacity calculated according to Privalov and Potekhin (1986). In the denaturation range considered, $<\Delta H>$ profiles depend on the scan rate, i.e. at $T = T_i$, $<\Delta H>_{T=Ti}$ is a function of the scan rate. For a first-order process, the relationship between $<\Delta H>$, $<\Delta H>_{rev}$, T and v is given by the following equation (Freire et al. 1987):

$$(\Delta H - \langle \Delta H \rangle) = \left(\Delta H - \langle \Delta H \rangle_{rev}\right) \exp\left(-\frac{1}{v} \int_{T_0}^{T} k_{app} \mathrm{d}t \right) \tag{2}$$

where ΔH is the calorimetric enthalpy calculated at the chosen scan rate, $<\Delta H>_{rev}$ represents the cumulative enthalpy function containing the information pertinent only to the species that are in thermodynamic equilibrium, and k_{app} is the apparent kinetic constant. Obviously, when v tends to ∞, $<\Delta H>$ tends to $<\Delta H>_{rev}$ exponentially.

In Fig. 3a we show the experimental and the extrapolated Cp_{exc} curve at infinite scan rate according to the procedure described above, which represents the reversible component of the amicyanin thermal unfolding. From this curve it is possible to obtain $\Delta H_U = 331 \pm 11$ kJ mol^{-1} and $T_{1/2} = 74.73 \pm 0.06$ °C (see Table 1). According to the van't Hoff ratio (Privalov 1982) reported in Table 1, this is a classical "all-or-none" equilibrium.

In previous papers concerning the thermal studies of azurin (La Rosa et al. 1995) and plastocyanin (Milardi et al. 1996), two small blue copper proteins with structural features similar to amicyanin, the path of unfolding of both proteins was depicted according to the Lumry and Eyring (Lumry and Eyring 1954; Sanchez-Ruiz 1992) model $N \rightleftharpoons U \rightarrow F$, where N, U and F are the native, unfolded and final states, respectively. Any attempt to fit the amicyanin DSC profiles with this model failed. On the other hand, the complexity of either the DSC or fluorescence data indicate that the thermal unfolding of this protein must involve more than two steps.

In this respect, two possible models have been considered. Model A:

$$\begin{array}{ccccc} N & \underset{\Delta H_U}{\overset{K}{\rightleftharpoons}} & U & \xrightarrow[}{k_1, Q_1} & F_1 \\ & & \downarrow_{Q_2, k_2} & & \\ & & F_2 & & \end{array} \tag{3}$$

and model B:

$$N \underset{\Delta H_U}{\overset{K}{\rightleftharpoons}} U \xrightarrow[Q_1]{k_1} F_1 \xrightarrow[Q_2]{k_2} F_2 \tag{4}$$

where, in both schemes, K is the thermodynamic equilibrium constant associated with the reversible step:

$$K = \exp\left[-\frac{\Delta H_U}{R}\left(\frac{1}{T}-\frac{1}{T_{1/2}}\right)\right] \quad (5)$$

where ΔH_U is the unfolding enthalpy, $T_{1/2}$ is the temperature at which $K=1$ and R is the gas constant. The k_i terms refer to the kinetic constants of the irreversible steps:

$$k_i = \exp\left[-\frac{E_{att}}{R}\left(\frac{1}{T}-\frac{1}{T^*}\right)\right] \quad (6)$$

where E_{att} is the activation energy associated with the irreversible steps, T^* is the temperature at which $k_i=1$ and R has its usual meaning. According to model A (Eq. 3), the native state (N) is in equilibrium with the unfolded state (U) which can undergo two simultaneous irreversible transformations into states F_1 and F_2. One of these two irreversible processes is exothermic. According to model B (Eq. 4), after the N⇌U step, an irreversible transformation of the unfolded state to the F_1 state occurs. Finally, F_1 approaches irreversibly the final F_2 state. This last step is exothermic. To choose the best model describing the thermal denaturation of amicyanin, it is necessary to derive the expression of Cp_{exc} for the models A and B to be used for the simulation of the experimental curves. The mathematical details to derive the Cp_{exc} expressions of the two models are given in the Appendix. In order to verify which model is able to better describe the thermal unfolding of amicyanin, the experimental Cp_{exc} profiles obtained at different scan rates were fitted using (see Appendix) Eq. (A12) representing model A and Eq. (B9) describing model B.

Figure 6a and b shows the fit of the experimental DSC profile recorded at 0.5 K min^{-1} using the A (Fig. 6a) or B (Fig. 6b) model. It is evident that only model B reproduces the experimental data in the whole temperature range with a high degree of accuracy. The parameters obtained from the simulations of all DSC profiles with models A and B are given in Table 2.

As already pointed out, the ΔCp value of amicyanin cannot be determined experimentally, because the value of Cp at the offset temperature must be ascribed to the final state and not to the unfolded state; hence, other methods should be used. The experimental method based on DSC measurements at different pH cannot be applied in our case because amicyanin is stable over only a narrow pH range. Thus, ΔCp had to be calculated using two different theoretical methods (Murphy and Gill 1991; Milardi et al. 1997). Both are based on the primary structure of the protein and, in addition, the second one includes a temperature dependence of ΔCp (Milardi et al. 1997). The first approach consists in the use of the Murphy and Gill model (Murphy and Gill 1991). According to this model, the ΔCp value can be evaluated on the basis of the following set of equations:

$$\Delta Cp = \Delta Cp_{ap} + \Delta Cp_{pol} \quad (7)$$

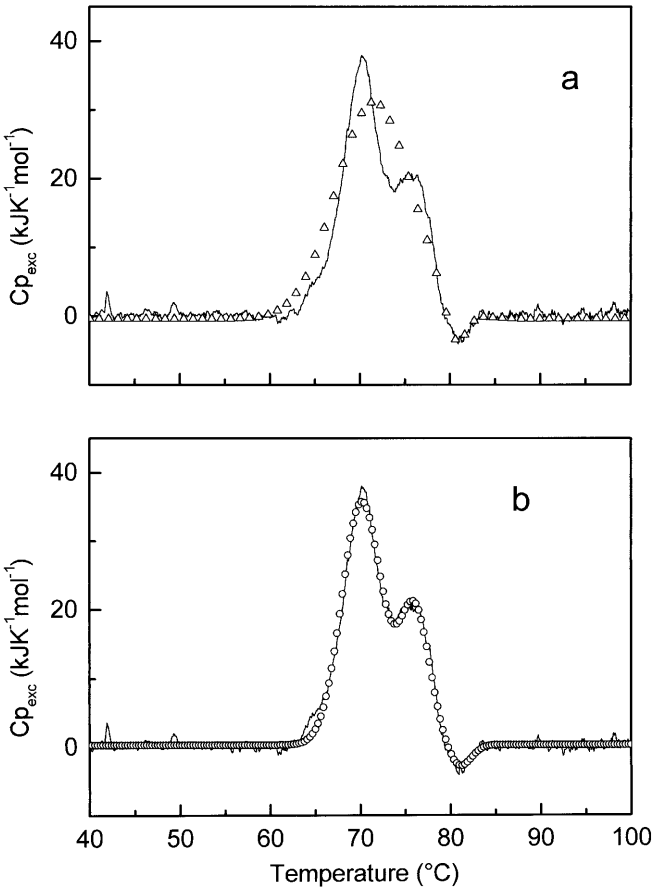

Fig. 6 Curve fitting of the experimental Cp_{exc} profile (*solid line*) recorded at 0.5 K min^{-1} with **a** model A and **b** model B (*open circles*)

$$\Delta Cp_{ap} = f_{ap} \times N_{CH} \times \Delta C^0_{p,CH} \quad (8)$$

$$f_{ap} = 0.574 + 0.000702 \times N_{res} \quad (9)$$

$$\Delta C_{p,pol} = 0.73 \times N_{res} \times \Delta C^0_{p,-CONH-} \quad (10)$$

$$\Delta C^0_{p,-CONH-} = -60 \pm 6 \text{ J K}^{-1} \text{ mol}^{-1} \quad (11)$$

$$\Delta C^0_{p,-CH-} = 28 \pm \text{ J K}^{-1} \text{ mol}^{-1} \quad (12)$$

where ΔCp_{ap} is the denaturational heat capacity change ascribable to apolar groups, ΔCp_{pol} is the heat capacity change ascribable to polar groups, f_{ap} is the fraction of apolar buried surface area, N_{res} is the number of the residues in the protein, N_{CH} is the number of apolar hydrogen atoms (i.e., the hydrogen atoms directly bound to a carbon atom), $\Delta C^0_{p,-CH-}$ is the specific contribution of one mole of apolar hydrogens to the overall denaturational heat capacity change and $\Delta C^0_{p,-CONH-}$ is the specific contribution ascribable to one mole of polar residues. As there are 643 apolar hydrogen atoms and 106 amino acid residues in amicyanin, the ΔCp value calculated for amicyanin is 7.03 kJ K^{-1} mol^{-1}.

Table 2 Parameters obtained for the two time-dependent unfolding steps of models A and B as derived from the curve fitting operations carried out on DSC curves at different scan rates (see description in the text). Enthalpy and activation energies are given in kJ mol^{-1}, temperature values in °C, scan rates in K min^{-1}. The minimum increments in the minimization procedure are 1 kJ mol^{-1} for the enthalpies, 0.1 °C for the temperatures. During the fitting operation, K (which in turn depends on ΔH_U and $T_{1/2}$) is constant. On the other hand, k_1 and k_2 (the kinetic constants which depend on E_1, T_1* and E_2, T_2*, respectively) are freely floating. The irreversibly reached states F_1 and F_2, as observed for azurin and plastocyanin in the above-mentioned papers, are a complex family of different conformers whose relative populations is dependent on the scan rate. As a consequence, the kinetic parameters E_1, E_2, T_1* and T_2* result in being scan rate dependent

Model A

	U→F$_1$			U→F$_2$			m[a]
v (K min^{-1})	E_1 (kJ mol^{-1})	T_1^* (°C)	ΔH_{F1} (kJ mol^{-1})	E_2 (kJ mol^{-1})	T_2^* (°C)	ΔH_{F2} (kJ mol^{-1})	
0.3	190	70.8	–201.0	504.3	75	10	83
0.5	127.3	71.2	–230.7	432.1	76	40.6	47
0.7	147.2	75.2	–200.5	401.1	79.4	37.6	90
1	101.8	79.8	–215.8	375.3	80.1	49.1	75

Model B

	U→F$_1$			F$_1$→F$_2$			m[a]
v (K min^{-1})	E_1 (kJ mol^{-1})	T_1^* (°C)	ΔH_{F1} (kJ mol^{-1})	E_2 (kJ mol^{-1})	T_2^* (°C)	ΔH_{F2} (kJ mol^{-1})	
0.3	160.4	59.1	–131.5	414.2	75.2	94.2	16
0.5	139.8	62.4	–130.5	401.5	76.7	103.3	8
0.7	121.2	71.2	–131.1	392.1	80.0	100.1	15
1	101.8	77.9	–101.9	381.5	81.2	82.3	11

[a] m (kJ K^{-1} mol^{-1}) is a measure of the accuracy of the fitting operation. It is defined as: $m = \frac{\sum_i |Cp^i_{theor} - Cp^i_{exp}|}{n}$, where Cp^i_{exp} is the ith value of the experimental Cp thermogram, Cp^i_{theor} is the corresponding calculated value and n is the total number of points of the scan

The second approach, developed by some authors of the present work (Milardi et al. 1997), is based on the averaging property of globular proteins. Considering that the apolar components of ΔCp_{ap} for proteins is a linear function of temperature:

$$\begin{aligned}\Delta Cp_{ap}(T) &= a + bT \\ &= (-2.43877 + 0.023205 \times N_{CH}) \\ &\quad + (0.00155241 - 4.89819 \times 10^{-5} \times N_{CH})\end{aligned} \tag{13}$$

the polar components of ΔCp_{pol} do not vary linearly with temperature, but follow a parabolic trend:

$$\Delta Cp_{pol}(T) = \alpha + \beta T + \gamma T^2 \tag{14}$$

where α, β and γ are given by:

$$\alpha = 1.5563 - 0.0684997 \times N_{res} \tag{15}$$

$$\beta = -0.0599115 + 0.000867265 \times N_{res} \tag{16}$$

$$\gamma = 0.000429975 - 5.24539 \times 10^{-6} N_{res} \tag{17}$$

Thus the $\Delta Cp(T)$ as a function of the temperature for a globular protein with a known number of apolar hydrogen (N_{CH}) and number of amino acid residues (N_{res}) can be obtained from the following equation:

$$\Delta Cp(T) = (a + \alpha) + (b + \beta)T + \gamma T^2 \tag{18}$$

For amicyanin, the ΔCp value in the investigated temperature range can be considered slightly dependent on temperature and is, on average, 6.75 kJ K^{-1} mol^{-1}. The average of the two values calculated by means of the two different methods was 6.88 ± 0.2 kJ K^{-1} mol^{-1}, and this value was adopted for the calculation of the denaturation Gibbs free energy (ΔG) of the protein in the 0–100 °C temperature range shown in Fig. 7.

Conclusively, the integrated use of DSC, EPR, CD, optical and fluorescence data has made it possible to highlight fundamental aspects concerning both the energetics and the thermal unfolding mechanism of amicyanin. The thermal denaturation of this protein is a complex process in which at least two intermediate states are populated. The DSC behaviour parallels the thermal effects observed by the fluorescence emission of the single Trp residue of the protein. The irreversible changes in the copper environment are observed after

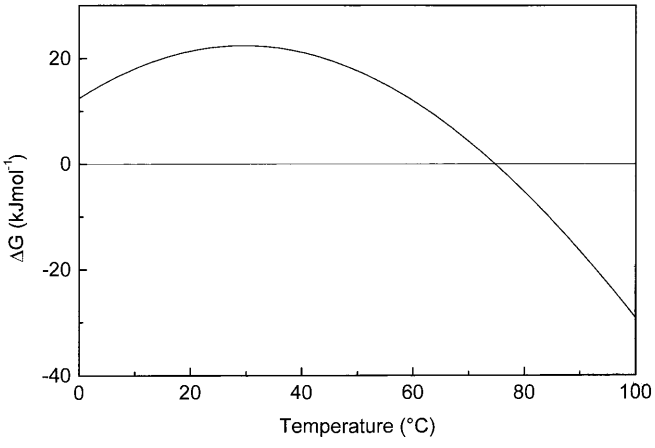

Fig. 7 Gibbs free energy of denaturation as a function of temperature for amicyanin

the first DSC peak once the disruption of the β-sheet structure of the protein starts.

The equilibrium step of the unfolding mechanism of amicyanin has been separated from the irreversible ones by means of the extrapolation of the Cp_{exc} at infinite scan rate (data reported in Table 1). This procedure has allowed us to calculate the thermodynamic stability of amicyanin in the 0–100 °C range.

Acknowledgements This work was financially supported by MURST (Ministero della Università e della Ricerca Scientifica e Tecnologica) and the University of Catania. One of us (R.G.) thanks the INFM (Istituto Nazionale di Fisica della Materia) for a post-doctoral fellowship. Thanks are due to Mrs. G. Warmerdam and E. de Waal for assisting in the protein purification.

Appendix

Model A

The rate equations for the irreversible formation of F_1 and F_2 from U are:

$$\begin{aligned}\frac{dx_{F_1}}{dT} &= \frac{1}{v}k_1 x_U \\ \frac{dx_{F_2}}{dT} &= \frac{1}{v}k_2 x_U\end{aligned} \tag{A1}$$

where x_{F1} and x_{F2} are the molar fractions of the two final states and v is the heating rate ($v = dT/dt$).

By combining the expression for the equilibrium constant ($K = x_U/x_N$) with x_U and x_N, the molar fractions of the unfolded and native state, respectively, and the conservation of mass ($x_N + x_U + x_{F1} + x_{F2} = 1$), it can be easily deduced that $x_U = K(1–x_{F1}–x_{F2})/(K+1)$.

The two equations A1 can be written as:

$$\begin{aligned}\frac{dx_{F_1}}{dT} &= \frac{1}{v}\frac{k_1 K}{K+1}(1 - x_{F_1} - x_{F_2}) \\ \frac{dx_{F_2}}{dT} &= \frac{1}{v}\frac{k_2 K}{K+1}(1 - x_{F_1} - x_{F_2})\end{aligned} \tag{A2}$$

By solving the differential equations system, we will obtain the temperature dependence of x_{F1} and x_{F2} for a DSC experiment.

If it is supposed that the irreversible steps occur with a non-negligible thermal effect Q_1 and Q_2, in particular $\Delta H = \Delta H_U + Q_1 + Q_2$, the average excess enthalpy can therefore be expressed as $\langle \Delta H \rangle = x_U \Delta H_U + x_F 1(\Delta H_U + Q_1) + x_F 2(\Delta H_U + Q_2)$, or, keeping in mind that $x_N + x_U + x_F 1 + x_F 2 = 1$, as $\langle \Delta H \rangle = \Delta H_U(x_U + x_F 1 + x_F 2) + Q_1 x_F 1 + Q_2 x_F 2$ or $\langle \Delta H \rangle = \Delta H_U(1 - x_N) + Q_1 x_F 1 + Q_2 x_F 2$.

The Cp_{exc} profile is given by:

$$Cp_{exc} = \frac{d\langle \Delta H \rangle}{dT} = \frac{d}{dT}[\Delta H_U(1 - x_N)] + Q_1\frac{dx_{F_1}}{dT} + Q_2\frac{dx_{F_2}}{dT} \tag{A3}$$

If Eq. (A3) is taken into account, the system of Eq. (A2) can be solved as follows:

$$\frac{dx_{F_1}}{dT} + \frac{dx_{F_2}}{dT} = \frac{1}{v}\frac{K(k_1 + k_2)}{K+1}(1 - x_{F_1} - x_{F_2}) \tag{A4}$$

Setting $x_{F1} + x_{F2} = u$ we obtain $dx_{F1} + dx_{F2} = du$ and substituting these equations into Eq. (A4) we obtain:

$$\frac{du}{dT} = \frac{1}{v}\frac{K(k_1 + k_2)}{K+1}(1 - u) \tag{A5}$$

By integration of differential equation (A5) from a low temperature T_0 (at which the reactions rate is negligible and $x_{F1} = 0$ and $x_{F2} = 0$), to a temperature T we obtain:

$$u = 1 - \exp\left[-\frac{1}{v}\int_{T_0}^{T}\frac{K(k_1 + k_2)}{K+1}dT\right] \tag{A6}$$

By substituting the solution (A6) into system (A2) we obtain:

$$\frac{dx_{F_1}}{dT} = \frac{1}{v}\frac{Kk_1}{K+1}\exp\left[-\frac{1}{v}\int_{T_0}^{T}\frac{K(k_1 + k_2)}{K+1}dT\right] \tag{A7}$$

$$\frac{dx_{F_2}}{dT} = \frac{1}{v}\frac{Kk_2}{K+1}\exp\left[-\frac{1}{v}\int_{T_0}^{T}\frac{K(k_1 + k_2)}{K+1}dT\right] \tag{A8}$$

$$x_U = \frac{K}{K+1}\exp\left[-\frac{1}{v}\int_{T_0}^{T}\frac{K(k_1 + k_2)}{K+1}dT\right] \tag{A9}$$

$$x_N = \frac{x_U}{K} = \frac{1}{K+1}\exp\left[-\frac{1}{v}\int_{T_0}^{T}\frac{K(k_1 + k_2)}{K+1}dT\right] \tag{A10}$$

and, as a consequence:

$$\frac{dx_N}{dT} = -\frac{K}{(K+1)^2}\left(\frac{k_1 + k_2}{v} + \frac{\Delta H_U}{RT^2}\right) \times \exp\left[-\frac{1}{v}\int_{T_0}^{T}\frac{K(k_1 + k_2)}{K+1}dT\right] \tag{A11}$$

Substituting Eqs. (A4), (A8) and (A11) into Eq. (A3), we obtain the expression for the Cp_{exc} describing model A:

$$Cp_{\mathrm{exc}} = \left\{ \frac{\Delta H_{\mathrm{U}} K}{K+1} \left(\frac{k_1 + k_2}{v} + \frac{\Delta H_{\mathrm{U}}}{RT^2} \right) + \left(\frac{Q_1 k_1 + Q_2 k_2}{v} \right) \left(\frac{K}{K+1} \right) \right\} \times \exp \left[-\frac{1}{v} \int_{T_0}^{T} \frac{K(k_1 + k_2)}{K+1} \mathrm{d}T \right] \tag{A12}$$

It is interesting to note that by setting the scan rate $v = \infty$, Eq. (A12) reduces to the equation describing a two-state reversible model.

Model B

In this case, the rate equations for the irreversible formation of F_1 and F_2 from U are:

$$\begin{aligned} \frac{\mathrm{d}x_{\mathrm{F}_1}}{\mathrm{d}T} &= \tfrac{1}{v}(k_1 x_{\mathrm{U}} - k_2 x_{\mathrm{F}_1}) \\ \frac{\mathrm{d}x_{\mathrm{F}_2}}{\mathrm{d}T} &= \tfrac{1}{v} k_2 x_{\mathrm{F}_1} \end{aligned} \tag{B1}$$

and, taking into account that $x_N + x_U + x_F 1 + x_F 2 = 1$, and the expression for the equilibrium constant $K = x_U / x_N$, then:

$$x_{\mathrm{U}} = \left(\frac{K}{K+1} \right) (1 - x_{\mathrm{F}_1} - x_{\mathrm{F}_2}) \tag{B2}$$

By substituting Eq. (B2) into system (B1):

$$\begin{aligned} \frac{\mathrm{d}x_{F1}}{\mathrm{d}T} &= \tfrac{1}{v} \left[\left(\tfrac{K}{K+1} \right) (1 - x_{\mathrm{F}_1} - x_{\mathrm{F}_2}) - k_2 x_{\mathrm{F}_1} \right] \\ \frac{\mathrm{d}x_{\mathrm{F}_2}}{\mathrm{d}T} &= \tfrac{1}{v} k_2 x_{\mathrm{F}_2} \end{aligned} \tag{B3}$$

The solution of the system (B3) was done by using the same technique used to solve the system (A2). Integrating from T_0, at which $x_{\mathrm{F}1} = 0$, to T we obtain:

$$x_{\mathrm{F}_1} = \frac{1}{v} \left[\exp \left(-\frac{1}{v} \int_{T_0}^{T} k_2 \mathrm{d}T \right) \right] \times \int_{T_0}^{T} \frac{k_1 K}{K+1} \exp \left(-\frac{1}{v} \int_{T_0}^{T} \frac{K(k_1 + k_2) + k_2}{K+1} \mathrm{d}T \right) \mathrm{d}T \tag{B4}$$

By substituting (B4) into the second equation of the system (B3) and integrating from T_0, at which $x_{\mathrm{F}2} = 0$, to T we obtain:

$$x_{\mathrm{F}_2} = \frac{1}{v^2} \left[\int_{T_0}^{T} k_2 \exp \left(-\frac{1}{v} \int_{T_0}^{T} k_2 \mathrm{d}T \right) \times \int_{T_0}^{T} \frac{k_1 K}{K+1} \exp \left(-\frac{1}{v} \int_{T_0}^{T} \frac{K(k_1 + k_2) + k_2}{K+1} \mathrm{d}T \right) \mathrm{d}T \right] \mathrm{d}T \tag{B5}$$

Finally, taking into account that $K = x_U / x_N$:

$$x_{\mathrm{U}} = \frac{K}{K+1} \exp \left(-\frac{1}{v} \int_{T_0}^{T} \frac{K k_1}{K+1} \mathrm{d}T \right) \tag{B6}$$

$$x_{\mathrm{N}} = \frac{1}{K+1} \exp \left(-\frac{1}{v} \int_{T_0}^{T} \frac{K k_1}{K+1} \mathrm{d}T \right) \tag{B7}$$

the cumulative enthalpy is given by $\langle \Delta H \rangle = x_U \Delta H_U + x_F 1 (\Delta H_U + Q_1) + x_F 2 (\Delta H_U + Q_1 + Q_2)$. Taking into account the mass conservation law and deriving $< \Delta H >$ with respect to the temperature, the Cp_{exc} function is obtained:

$$\begin{aligned} Cp_{\mathrm{exc}} &= \frac{\mathrm{d}\langle \Delta H \rangle}{\mathrm{d}T} \\ &= \frac{\mathrm{d}}{\mathrm{d}T} [\Delta H_{\mathrm{U}} (1 - x_{\mathrm{N}})] + \frac{\mathrm{d}}{\mathrm{d}T} [Q_1 (x_{\mathrm{F}_1} - x_{\mathrm{F}_2})] + Q_2 \frac{\mathrm{d}x_{\mathrm{F}_2}}{\mathrm{d}T} \end{aligned} \tag{B8}$$

If the first derivative with respect to the temperature of the Eqs. (B4), (B5), (B6) and (B7) are substituted into Eq. (B8), we can obtain the expression for the Cp_{exc} for model B:

$$Cp_{\mathrm{exc}} = \left[\frac{K \Delta H}{(K+1)^2} \left(\frac{k_1}{v} + \frac{\Delta H}{RT^2} \right) + \frac{Q_1}{v} \frac{k_1 K}{K+1} \right] \times \exp \left(-\frac{1}{v} \int_{T_0}^{T} \frac{K k_1}{K+1} \mathrm{d}T \right) + \Lambda(v, T) \tag{B9}$$

where $\Lambda(v,T)$ is:

$$\Lambda(v,T) = \frac{Q_2 k_2}{v^2} \exp \left(-\frac{1}{v} \int_{T_0}^{T} k_2 \mathrm{d}T \right) \times \int_{T_0}^{T} \frac{k_1 K}{K+1} \exp \left(-\frac{1}{v} \int_{T_0}^{T} \frac{K(k_1 + k_2) + k_2}{K+1} \mathrm{d}T \right) \mathrm{d}T \tag{B10}$$

It is interesting to note that the first term on the right-hand side of Eq. (B9) represents the Cp_{exc} for the Lumry and Eyring model; this solution can be obtained by setting $k_2 = 0$. Moreover, by setting $v = \infty$, Eq. (B9) reduces to the equation describing a two-state reversible model.

References

Abkevich VI, Gutin AM, Shakhnovich EI (1995) Domains in folding of model proteins. Protein Sci 4:1167–1177

Addison AW (1983) Spectroscopic and redox trends from model copper complexes. In: Karlin KD, Zubieta J (eds) Copper coordination chemistry: biochemical & inorganic perspectives. Adenine Press, Guilderland, New York, pp 109–128

Bohm G, Muhr R, Jaenicke R (1992) Quantitative analysis of protein far UV circular dichroism spectra by neural networks. Protein Eng 5:191–195

Dobson CM (1995) Finding the right fold. Nat Struct Biol 2:513–517

Fee JA (1975) Copper proteins – systems containing a "blue" copper center. In: Dunitz JD, Hemmerich P, Holm RH, Ibers JA, Jorgensen CK, Neilands JB, Reinen D, Williams RJP (eds) Structure and Bonding, vol 23. Springer, Berlin Heidelberg New York, pp 1–53

Freire E, Van Odsol WW, Mayorga OL, Sanchez-Ruiz JM (1987) Calorimetrically determined dynamics of complex unfolding transition in proteins. Annu Rev Biophys Chem 38:463–479

Garel JR (1992) Folding of large proteins: multidomain and multisubdomain proteins. In: Creighton TE (ed) Protein folding. Freeman, New York, pp 405–454

Hennessey JP, Johnson WC (1981) Information content in the circular dichroism of proteins. Biochemistry 20:1085–1094

Husain M, Davidson VL (1985) An inducible periplasmic blue copper protein from *Paracoccus denitrificans*. Purification, properties, and physiological role. J Biol Chem 260:14626–14629

Jaenicke R (1991) Protein folding: local structures, domains, subunits, and assemblies. Biochemistry 30:3147–3161

Kalverda KP, Wymenga SS, Lommen A, Ven FJM van de, Hilbers CW, Canters GW (1994) Solution structure of the type 1 blue copper protein amicyanin from *Thiobacillus versutus*. J Mol Biol 240:358–371

La Rosa C, Grasso D, Milardi D, Guzzi R, Sportelli L (1995) Thermodynamics of the thermal unfolding of azurin. J Phys Chem 99:14864–14870

La Rosa C, Milardi D, Grasso D (1998) Thermodynamics and kinetics of globular protein thermal unfolding. Recent Res Dev Phys Chem 2:175–202

Lakowicz JR (1983) Principles of fluorescence spectroscopy. Plenum Press, New York

Lawton SA, Anthony C (1985) The role of blue copper proteins in the oxidation of methylamine by an obligate methylotroph. Biochem J 228:719–726

Leckner J, Bonander N, Wittung-Stafshede P, Malmstrom BG, Karlsson G (1997) The effect of the metal ion on the folding energetics of azurin: a comparison of the native, zinc and apoprotein. Biochim Biophys Acta 1342:19–27

Lumry R, Eyring H (1954) Conformation changes of proteins. J Phys Chem 58:110–120

Malkin R, Malmstrom BG (1970) The state and function of copper in biological systems. Adv Enzymol 33:177–182

Manalevan P, Johnson WC (1987) Variable selection method improves the prediction of protein secondary structure from circular dichronism spectra. Anal Biochem 167:76–85

Milardi D, Fasone S, La Rosa C, Grasso D (1996) Contribution of polar and apolar groups to the thermodynamic stability of azurin. Nuovo Cimento 18:1347–1353

Milardi D, La Rosa C, Fasone S, Grasso D (1997) An alternative approach in the structure-based prediction of the thermodynamics of protein unfolding. Biophys Chem 69:43–51

Milardi D, La Rosa C, Grasso D, Guzzi R, Sportelli L, Fini C (1998) Thermodynamics and kinetics of the thermal unfolding of plastocyanin. Eur Biophys J 27:273–282

Murphy PK, Gill SJ (1991) Solid model compounds and the thermodynamics of protein unfolding. J Mol Biol 222:699–709

Novokhatny VV, Madved LV, Kudinov SA, Privalov PL (1984) Domains in human plasminogen. J Mol Biol 179:215–232

Privalov PL (1982) Stability of proteins. Proteins which do not present a single cooperative system. Adv Protein Chem 35: 1–104

Privalov PL, Potekhin SA (1986) Scanning microcalorimetry in studying temperature-induced changes in proteins. Methods Enzymol 4:4–51

Provencher SW, Glöckner J (1981) Estimation of globular protein secondary structure from circular dichroism. Biochemistry 20:33–37

Ptitsyn OB (1992) The molten globule state. In: Creighton TE (ed) Protein folding. Freeman, New York, pp 243–300

Romero A, Nar H, Huber R, Messerschmidt A, Kalverda AP, Canters GW, Durley R, Mathews FS (1994) Crystal structure analysis and refinement at 2.15 Å resolution of amicyanin, a type I blue copper protein, from *Thiobacillus versutus*. J Mol Biol 236:1196–1211

Sanchez-Ruiz JM (1992) Theoretical analysis of Lumry-Eyring models in differential scanning calorimetry. Biophys J 61:921–935

Sreerama N, Woody RW (1994) Protein secondary structure from circular dichroism spectroscopy. Combining variable selection principle and cluster analysis with neural network, ridge regression and self-consistent methods. J Mol Biol 242:497–507

Tanford C (1968) Protein denaturation. Adv Protein Chem 23:121–275

Tobari JC (1984) Blue copper proteins in electron transport of methylotropic bacteria. In: Crawford RL, Hanson RS (eds) Microbial growth on C1 compounds. American Society for Microbiology, Washington, pp 106–112

Tobari J, Harada Y (1981) Amicyanin: an electron acceptor of methylamine dehydrogenase. Biochem Biophys Res Commun 101:502–508

Van Houwelingen T, Canters GW, Stobbelaar G, Duine JA, Frank J, Tsugita A (1985) Isolation and characterization of a blue copper protein from *Thiobacillus versutus*. Eur J Biochem 153:75–80

Wetlaufer DB (1973) Nucleation, rapid folding, and globular intrachain regions in proteins. Proc Natl Acad Sci USA 70:697–701